RJC

RASĀYAN *J. Chem.*
238-244| Special Issue | 2021
ISSN: 0974-1496 | e-ISSN: 0976-0083 | CODEN: RJCABP
http://www.rasayanjournal.com
http://www.rasayanjournal.co.in

ANTICORROSIVE EVALUATION OF COPPER-IRON MIXTURES PROCESSED BY POWDER METALLURGY

W. Aperador[1,✉], J. Bautista-Ruiz[2] and J.C. Caicedo[3]
[1]Faculty of Engineering, Universidad ECCI, Bogotá, Colombia, 11101.
[2]Faculty of Engineering, Universidad Francisco de Paula Santander, San José de Cúcuta, Colombia, 540005.
[3] Faculty of Engineering, Universidad del Valle, Cali, Colombia, 760034.
✉Corresponding Author: g.ing.materiales@gmail.com

ABSTRACT

Through the powder metallurgy process, copper and iron powders were mixed in the proportions Cu between 15% to 75% and iron from 25% to 85% that made up the binary material systems. Material systems were topographically characterized with atomic force microscopy. Corrosion tests were established using potentiodynamic polarization curves. The worn surfaces' characterization was carried out by means of a Confocal Scanning Laser Microscope to complement the study. It was determined that the mixtures' stability and behaviour have different behaviours depending on the evaluated system because the wear system caused, indicating that the phenomenon can be additive. The corrosive phenomenon is dominantly affected by the microstructure of the material. From the results found, it is possible to infer that the best systems evaluated by corrosive contain the highest percentage of copper content. The topographic variation indicates the transition from the active zone to the passive zone of the metal due to electrochemical reactions in the presence of aggressive media.

Keywords: Powder Metallurgy, Copper, Iron, Corrosion, Roughness

RASĀYAN *J. Chem.*, *Special Issue*, 2021

INTRODUCTION

The powder metallurgical process is used to increase the pieces' mechanical resistance due to the high homogeneity and control of the size of the grains. By sintering, it is possible to join metallic alloys that are difficult to be combined (because they are refractory or because they have very different melting temperatures), allowing the production of parts from complex melting,forging, and machining materials.[1-4] The use of powder metallurgy has become popular on an industrial scale because it has allowed the development of advanced materials, obtaining metal parts that are difficult to manufacture with excellent tolerances, high quality, and series production.[5,6] The industrial application of the Fe-Cu binary alloy system covers sintered stainless steels such as different types of filters, ABS rings for automobiles. Also, in food industry equipment such as utensils, and kitchen accessories. This is because these elements have low resistance to corrosion due to interconnected porosity.[7-10] The powder metallurgical process depends on the characterization and metallic powder control.

The powder production method influences the particles morphology and the exact nature of the particle size distribution.[11] These properties also direct powders' behaviour during compaction and sintering and the composition, structure, and properties of the sintered material. Metallic powders must be considered raw material and not as a final product and produced, considering their application.[12]

Iron and copper mixtures increase the matrix's resistance, improve wear resistance, provide antifriction qualities, and resistance to atmospheric corrosion and chemical agents, especially in contact with sulfuric acid.[13] The hardening of iron due to the dissolution of copper in the crystalline lattice develops greater resistance and hardness. The consolidation of this type of material is carried out by an atypical cold pressing process and subsequent sintering.[14] Some research highlights that the Fe-Cu intermetallic compound has shown the best wear and corrosion properties by varying factors such as temperature, time, pressure, and chemical composition to obtain parts with the appropriate characteristics.[15-17] The effect of copper on steels improves mechanical resistance, provides good resistance to impact and abrasion. Copper has been used in

high-alloy and stainless steel to improve corrosion resistance. Copper has been used in stainless and high-alloy steels to improve corrosion resistance in specific environments, reduce susceptibility to stress corrosion cracking, and provide age hardening.[18-22]
In this research, iron and copper powders were used to modify the corrosion properties. For this purpose, the addition of copper powders in proportions of 15% - 75% of the alloying element was studied.

EXPERIMENTAL

Before the manufacturing process, an analysis of the powders was developed in its conditioning process, including the material's compaction and subsequent sintering. Iron and copper powders of 99.9% purity and particle size of ~ 80 μm was used in the conditioning process. The powders were mixed according to the following compositions Cu15% -Fe85%, Cu30% -Fe70%, Cu45% -Fe55%, Cu60% -Fe40%, Cu75% -Fe25%. The mechanical alloying was made in a hardened steel ball mill with a ball-powder weight ratio of 4:1.
A uniaxial force was applied to utilize a Universal Electromechanical Testing Machine type INSTRON model 4507 with a maximum load cell of 100 kN. The machine is equipped with a conventional resistance oven that allows working at maximum temperatures of 1300 °C. A mold was also used that allowed the controlled compaction of the material at 0.5 mm/s and a load of $7.1x10^3$ kgf/cm².
The powder falls by the gravitational force from the filling device into the mold cavity. The mold is provided with a cylindrical sleeve with a lower cover held by three screws. The punch was located inside the jacket and received the load employing a disk in charge of uniformly transporting the force of the Universal Machine to the powder. Therefore, its geometry was specific, and it was adapted to the upper plate of the machine.
The mixed powder material was processed in a uniaxial compression method. Subsequently, the compound was sintered, starting with a heating ramp up to 300 °C in 120 minutes. This temperature is that required for phase separation in solid polycrystalline Fe-Cu solutions. Then the ramp was raised for 120 minutes until reaching 500 °C, holding it for 120 minutes.
The damage produced by the effect of the corrosive fluid was determined using potentiodynamic polarization curves in a Princeton Applied Research™ Versastat II potentiostat-galvanostat equipment. An electrochemical cell configuration with three electrodes, a reference electrode (Ag/AgCl), a platinum counter electrode, and a working electrode for the analyzed sample was used. The working solution was 3.5% sodium chloride, simulating marine environment conditions. The potentiodynamic polarization curves were obtained at a scanning speed of 0.125 mV/s, a voltage ranges of -0.25 V to 0.25 V, and an exposure area of 1 cm^2. The sample was subjected to electrochemical measurement after immersion in test solution form 30 min at ambient temperature (20 °C) to obtain a stable state.
The surface evaluation was carried out at Confocal Laser Microscope Nikon C1 Plus ECLIPSE Ti. This technique required metallographic preparation of the specimen until dry polishing with abrasive papers number 2500 and dry cloth with diamond dust. As attack reagents, the following were used: a) 45 cm^3 of HCl, 15 cm^3 of HNO_3, and 20 cm^3 of ethanol.

RESULTS AND DISCUSSION

Figure-1 shows the potentiodynamic polarization curves for the five systems studied. It was found that systems with low concentrations tend to passivate with high current density and experienced widespread corrosion.[23] Materials with high percentages of copper showed general corrosion processes at the beginning, and from 130 mV (anodic region), there is an increase in current intensity that can be related to a high degree of porosity. Therefore, the formation of passivating corrosion products occurs at the beginning of the anodic zone, stabilizing rapidly. High values of anodic potentials can generate breaks in the passivating film. Repassivation is not evidenced, allowing corrosive attack by the presence of chlorides.[24]
Powder metallurgical materials made up of high percentages of copper in their composition have more positive potentials and low current densities. However, the samples of the Cu15%-Fe85% and Cu30%-Fe70% systems show similar corrosion potentials and currents. The systems Cu45%-Fe55%, Cu60%-Fe40%, and Cu75%-Fe25% showed more positive potentials depending on the amount of constitutive copper in the samples, but the current densities decreased. The behaviour is possibly due to the reaction of

copper with iron in the sintering process. In the cathode and anodic regions, fluctuations in the current density values are evidenced, indicating the existence of two or more reactions.

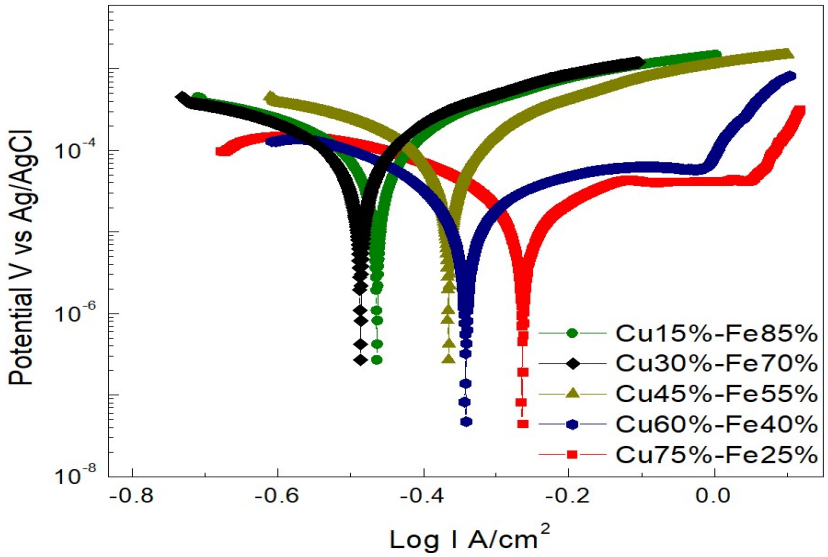

Fig.-1**:** Potentiodynamic Polarization Curves for the Systems Cu15%-Fe85%, Cu30%-Fe70%, Cu45%- Fe55%, Cu60%-Fe40% and Cu75%-Fe25% evaluated in Corrosion.

Figure-2 is the result of the analysis deterioration by corrosion. The potentiodynamic curves show that the mixtures generalized type corrosion due to the passive layers. This passive layer acts synergistically and inhibits the potentially damaging pitting corrosion process.[24] The materials obtained by powder metallurgy and evaluated for corrosion show lower corrosion rates. The Cu75%-Fe25% system decreased the corrosion rate values by two orders of magnitude. For the dual evaluation, the corrosion current density was $1.39x10^{-7}$ A/cm^2 and $1.74x10^{-5}$ A/cm^2 in the study of corrosion. Reducing the corrosion current is directly related to the corrosion rate decrease by increasing alloying iron percentage.[25] From the results found, it is possible to infer that the best systems evaluated by corrosive contain the highest percentage of copper content. This is due to physical-chemical conditions because copper metal oxides are stable to oxidation reactions with ions present in saline solution. Therefore, the corrosion rate values are related to the studied materials' chemical and mechanical reactions studied materials' chemical.

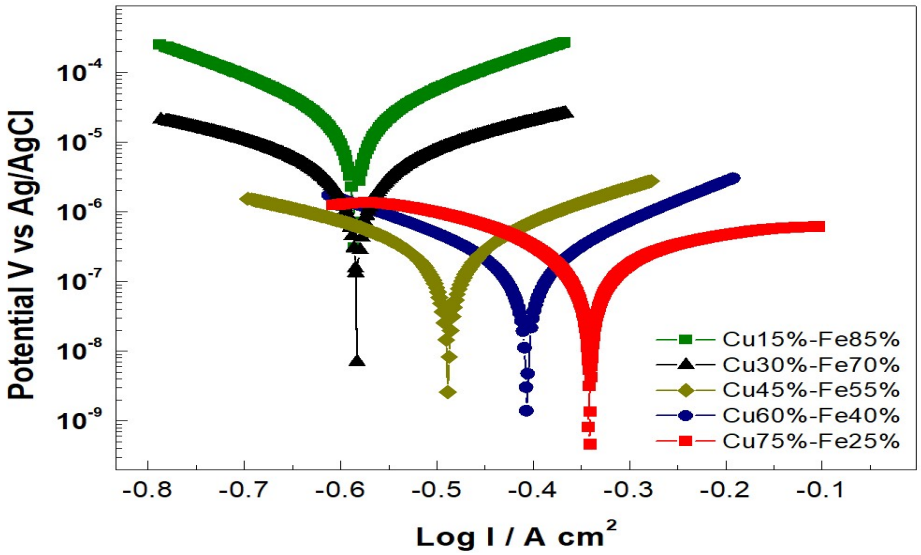

Fig.-2**:** Potentiodynamic Polarization Curves for the Systems Cu15%-Fe85%, Cu30%-Fe70%, Cu45%-Fe55%, Cu60%-Fe40% and Cu75%-Fe25% evaluated in Wear-corrosion.

Figure-3a, Fig.-3b, Fig.-3c, Fig.-3d and Fig.-3e shows the micrographs obtained by the atomic force microscopy technique. The micrographs were taken from the surface of the study materials after the mixing and sintering processes. The surfaces were polished with abrasive silicon carbide (SiC) papers with a granulometry of 220, 340, 400, 600, 1200, 1500, and 2000. The final metallographic gloss finish was given with a polishing machine and 0.05 μm alumina.

In the micrographs of Fig.-3, heterogeneous surfaces are observed. The roughness values were determined for each system studied, resulting in at 857 pm for the 15%Cu-85%Fe system, 848 pm for the 30%Cu-70%Fe system, 399 pm 45%Cu-55%Fe system, 175 pm for the 60%Cu-40%Fe system, and 129 pm for the 75%Cu-25%Fe system. In the two systems with greater roughness, pores are observed. In the other systems, smooth surfaces can be related to the powder metallurgical process, where the pressing process improves the adherence between the copper particles and facilitates the formation of bonds. Subsequently, the sintering process homogenizes and fuses the powders.

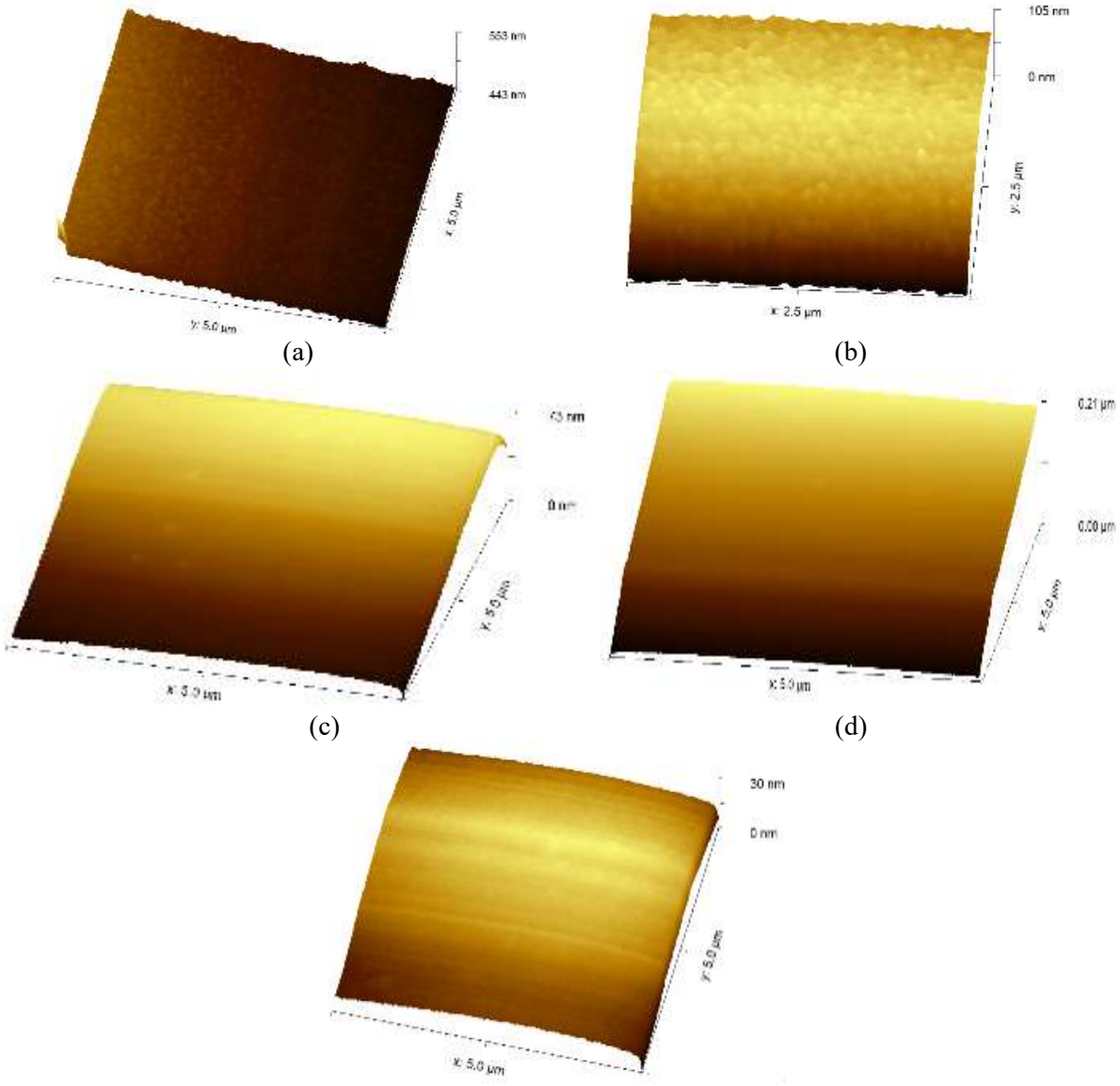

Fig.-3**:** AFM micrographs. (a) Cu15%-Fe85%, (b) Cu30%-Fe70%, (c) Cu45%-Fe55%, (d) Cu60%-Fe40% and (e) Cu75%-Fe25%.

Each material sample after the corrosion analysis was characterized by employing Confocal Laser Scanning Microscopy to determine the degree of damage suffered, as shown in Fig.-4. In Figure-4a, Fig.-4b and Fig.-4c the micrographs are observed for the systems Cu15%-Fe85%, Cu30%-Fe70% and Cu45%-Fe55%, respectively. Surface deterioration is evident due to corrosion with the formation of oxide layers. The topographic variation indicates the transition from the active zone to the passive zone of the metal due to electrochemical reactions in the presence of aggressive media such as 3.5% NaCl. Figure-4d and Fig.-4e correspond to the materials in compositions Cu60%-Fe40% and Cu75%-Fe25%. The study by potentiodynamic polarization curves allowed us to establish that these two compositions present the best anticorrosive performance.[26,27] However, as indicated, these two material systems show pitting corrosion due to the breakdown of the protective film due to chlorides' attack. These characteristics are revealed in the micrographs with greater deterioration in specific points like porous structures.

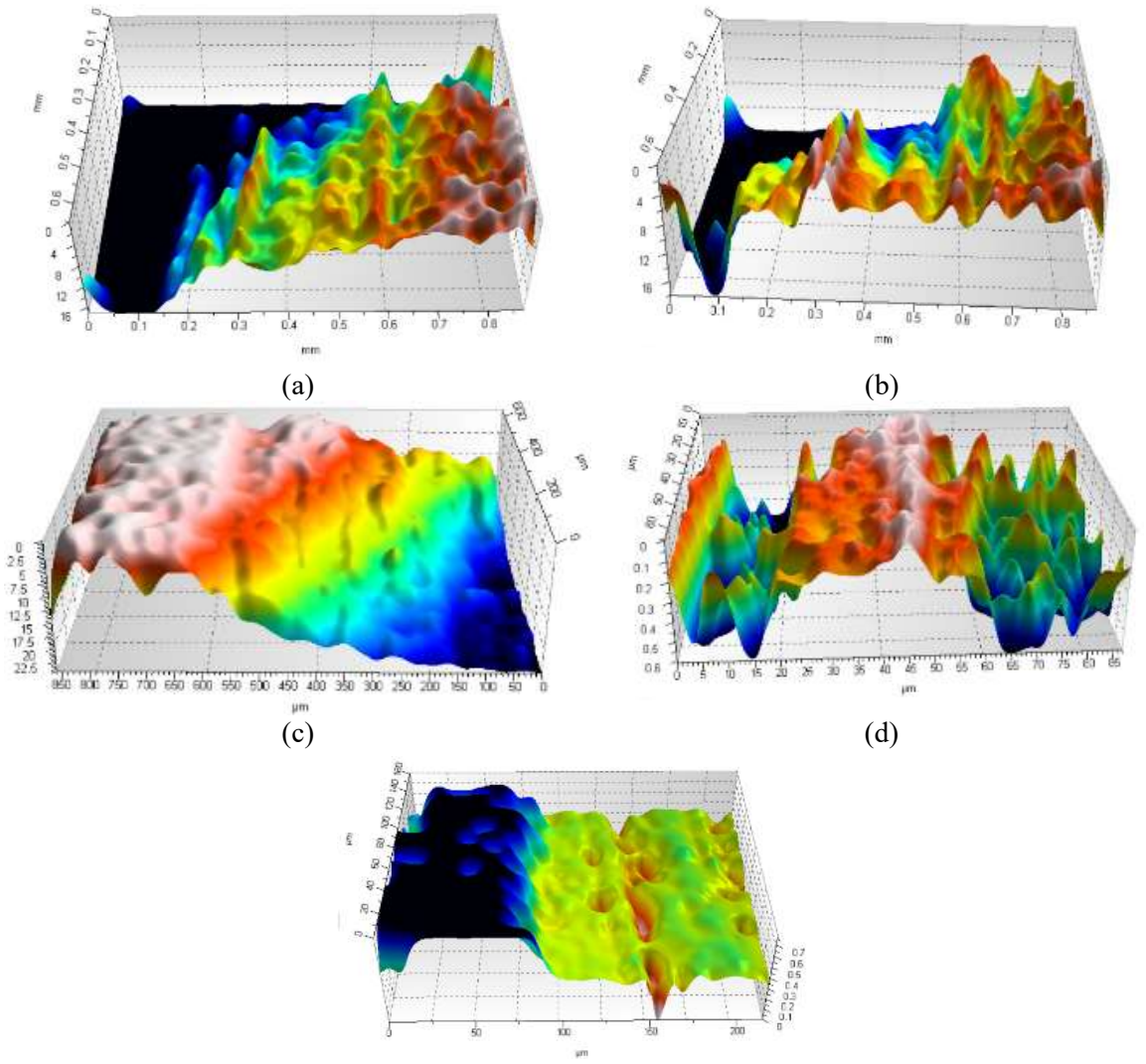

Fig.-4**:** Scanning Confocal Microscopy Micrographs. a) Cu15%-Fe85%, b) Cu30%-Fe70%, c) Cu45%-Fe55%, d) Cu60%-Fe40% and e) Cu75%-Fe25%.

CONCLUSION

From the results found, it is possible to infer that the best systems evaluated by corrosive contain the highest percentage of copper content. This is due to physicochemical conditions because copper metal oxides are stable to oxidation reactions with ions present in saline solution.

The smooth surfaces can be related to the powder metallurgical process, where the pressing process improves the adherence between the copper particles and facilitates the formation of bonds. Subsequently, the sintering process homogenizes and fuses the powders.

Each material sample after the corrosion analysis was characterized by employing Confocal Laser Scanning Microscopy to determine the degree of damage suffered Surface. The deterioration is evident due to corrosion with the formation of oxide layers. The topographic variation indicates the transition from the active zone to the passive zone of the metal due to electrochemical reactions in the presence of aggressive media.

REFERENCES

1. D. Chaira, *Science and Materials Engineering*, **2,** 588(2021), https://doi.org/10.1016/B978-0-12-803581-8.11703-5
2. A. Rodriguez-Contreras, M. Punset, J.A. Calero, F. Gil, E. Ruperez and J. Manero, *Journal of Materials Science & Technology*, **76**, 29(2021), https://doi.org/10.1016/j.jmst.2020.11.005
3. S. Jyothi, Y.V. Subba Rao and P.S. Ratnakumar, *Rasayan Journal of Chemistry,* **12(2)**, 537(2019), https://doi.org/10.31788/RJC.2019.1225000
4. J. Duan, M. Zang, P. Chen, Z. Li, L. Pang, P. Xiao and Y. Li, *Ceramics International,* **47(14),** 19271(2021), https://doi.org/10.1016/j.ceramint.2021.02.187
5. R. Thilagavathi, A. Prithiba and R. Rajalakshm, *Rasayan Journal of Chemistry*, **12(2)**, 431(2019), https://doi.org/10.31788/RJC.2019.1225133
6. D. Gu, Y. Shen, S. Fang and J. Xiao, *Journal of Alloys and Compounds*, **438(1–2)**, 184(2007), https://doi.org/10.1016/j.jallcom.2006.08.040
7. W. Hung-Kai, W. Zih-Huei and W. Ming-Chi, *Computers & Industrial Engineering,* **148**, 106635(2020), https://doi.org/10.1016/j.cie.2020.106635
8. J. Vairamuthu, B. Stalin, G.D. Sivakumar, B. Mohmed Fazil, R. Balaji and V.A. Natarajan, *Materials Today*, **45(2),** 1970 (2020), https://doi.org/10.1016/j.matpr.2020.09.262
9. E. Xu, J. Huang, Y. Li, Z. Zhu, M. Cheng, D. Li, H. Zhong, J. Liu and Y. Jiang, *Powder Technology,* **344**, 551(2019), https://doi.org/10.1016/j.powtec.2018.12.059
10. J. Bautista-Ruiz, W. Aperador and J.J. Olaya*, Rasayan Journal of Chemistry,* **11(2)**, 597(2018), https://doi.org/10.31788/RJC.2018.1122075
11. R. Groarke, A. A-Hameed, I.U.I. Ahad, R.K. Vijayaraghavan, A. O'Neill, P. McNally, Y. Delaure and D. Brabazon, *Materials & Design,* **182**, 108046(2019), https://doi.org/10.1016/j.matdes.2019.108046
12. A.H. Omran-Alkhayatt, S.M. Thahab, and I.A. Zgair, *Optik,* **127(8)**, 3745(2016), https://doi.org/10.1016/j.ijleo.2015.12.144
13. B.B. Vara Prasad, K.V. Ramesh and A. Srinivas, *Solid State Sciences,* **107**, 106325(2020), https://doi.org/10.1016/j.solidstatesciences.2020.106325
14. Y. Li, B. Yang, P. Zhang, Y. Nie, X. Yuan, Q. Lei and Y. Li, *Materials Today Communications*, **27**, 102266(2021), https://doi.org/10.1016/j.mtcomm.2021.102266
15. M.R. Akbarpour, H. Mousa Mirabad, M. Khalili Azar, K. Kakaei and H.S. Kim, *Materials Science and Engineering: A*, **786**, 139395(2020), https://doi.org/10.1016/j.msea.2020.139395
16. X. Ma, C. Luan, S. Fan, J. Deng, L. Zhang and L. Cheng, *Tribology International,* **154**, 106686(2021), https://doi.org/10.1016/j.triboint.2020.106686
17. Y. Bian, J. Ni, C. Wang, J. Zhen, H. Hao, X. Kong, H. Chen, J. Li, X. Li, Z. Jia, W. Luo and Z. Chen, *Materials Characterization,* **172**, 110847(2021), https://doi.org/10.1016/j.matchar.2020.110847
18. N. Ravikumar, T.R. Tamilarasan and R. Rajendran, *Carbon Trends,* **3**, 100031(2021), https://doi.org/10.1016/j.cartre.2021.100031
19. E.P. Shalunov and Y.O. Vladimirova, *Materials Today*, **38(4),** 1784(2021), https://doi.org/10.1016/j.matpr.2020.08.266
20. H. Zhou, P. Yao, Y. Xiao, K. Fan, Z. Zhang, T. Gong, L. Zhao, M. Deng, C. Liu and P. Ling, *Tribology International,* **132,** 199(2019), https://doi.org/10.1016/j.triboint.2018.11.027
21. M.R. Akbarpour, H. Mousa-Mirabad, M. Khalili Azar, K. Kakaei and H.S. Kim, *Materials Science and Engineering: A*, **786,** 139395(2020), https://doi.org/10.1016/j.msea.2020.139395

22. W. Yang, H. Zhao, K. Wang and C. Zheng, *Proceedings of the Combustion Institute*, **35,** 2811(2015), https://doi.org/10.1016/j.proci.2014.07.010
23. H. Torabi and R. Arghavanian, *Journal of Alloys and Compounds,* **806,** 99(2019), https://doi.org/10.1016/j.jallcom.2019.07.245
24. W. Yang, H. Zhao, K. Wang and C. Zheng, *Combustion Institute*, **35**, 2811(2015), https://doi.org/10.1016/j.proci.2014.07.010
25. L. Tan, Z. Wang, Y. Li, Y. Liu and F. Liu, *Materials Science and Engineering: A,* **800,** 140312(2021), https://doi.org/10.1016/j.msea.2020.
26. E. Kocaman, B. Kılınç, M. Durmaz, Ş. Şen and U. Şen, *Engineering Science and Technology, an International Journal,* **24(2),** 533(2021), https://doi.org/10.1016/j.jestch.2020.08.003.140312
27. P. Satishkumar, C. Saravana Murthi, R. Meenakshi and G. Ramesh, *Materials Today,* **37(2),** 3543(2021), https://doi.org/10.1016/j.matpr.2020.09.429

[RJC-6677/2021]